



## **Combining ibrutinib and checkpoint blockade improves CD8<sup>+</sup> T-cell function and control of chronic lymphocytic leukemia in E $\mu$ -TCL1 mice**

*by Bola S. Hanna, Haniyeh Yazdanparast, Yasmin Demerdash, Philipp M. Roessner, Ralph Schulz, Peter Lichter, Stephan Stilgenbauer, and Martina Seiffert*

*Haematologica 2020 [Epub ahead of print]*

*Citation: Bola S. Hanna, Haniyeh Yazdanparast, Yasmin Demerdash, Philipp M. Roessner, Ralph Schulz, Peter Lichter, Stephan Stilgenbauer, and Martina Seiffert. Combining ibrutinib and checkpoint blockade improves CD8<sup>+</sup> T-cell function and control of chronic lymphocytic leukemia in E $\mu$ -TCL1 mice. Haematologica. 2020; 105:xxx  
doi:10.3324/haematol.2019.238154*

### *Publisher's Disclaimer.*

*E-publishing ahead of print is increasingly important for the rapid dissemination of science. Haematologica is, therefore, E-publishing PDF files of an early version of manuscripts that have completed a regular peer review and have been accepted for publication. E-publishing of this PDF file has been approved by the authors. After having E-published Ahead of Print, manuscripts will then undergo technical and English editing, typesetting, proof correction and be presented for the authors' final approval; the final version of the manuscript will then appear in print on a regular issue of the journal. All legal disclaimers that apply to the journal also pertain to this production process.*

# **Combining ibrutinib and checkpoint blockade improves CD8<sup>+</sup> T-cell function and control of chronic lymphocytic leukemia in E $\mu$ -TCL1 mice**

Bola S. Hanna<sup>1</sup>, Haniyeh Yazdanparast<sup>1</sup>, Yasmin Demerdash<sup>1</sup>, Philipp M. Roessner<sup>1</sup>, Ralph Schulz<sup>1</sup>, Peter Lichter<sup>1</sup>, Stephan Stilgenbauer<sup>2</sup>, and Martina Seiffert<sup>1</sup>

<sup>1</sup>Molecular Genetics, German Cancer Research Center (DKFZ), Heidelberg, Germany

<sup>2</sup>Internal Medicine III, University of Ulm, Ulm, Germany

## **Contact information for correspondence:**

Martina Seiffert and Bola S. Hanna

Molecular Genetics (B060), German Cancer Research Center (DKFZ)

Im Neuenheimer Feld 280, 69120 Heidelberg, Germany.

Tel.: +49-6221-42 4586, Fax: +49-6221-42 4639

Email: [m.seiffert@dkfz.de](mailto:m.seiffert@dkfz.de) and [b.hanna@dkfz.de](mailto:b.hanna@dkfz.de)

**Keywords:** CLL, CD8<sup>+</sup> T-cells, ibrutinib, checkpoint blockade, combination

**Word count:** 4266

**Abstract:** 199

**References:** 49

**Figures/tables:** 6

**Running title:** Combining ibrutinib and checkpoint blockade in CLL

## Abstract

Ibrutinib is a bruton's tyrosine kinase (BTK) inhibitor approved for the treatment of multiple B-cell malignancies, including chronic lymphocytic leukemia (CLL). In addition to blocking B-cell receptor signaling and chemokine receptor-mediated pathways in CLL cells, that are known drivers of disease, ibrutinib also affects the microenvironment in CLL via targeting BTK in myeloid cells and IL-2-inducible T-cell kinase (ITK) in T-cells. These non-BTK effects were suggested to contribute to the success of ibrutinib in CLL. By using the E $\mu$ -TCL1 adoptive transfer mouse model of CLL, we observed that ibrutinib effectively controls leukemia development, but also results in significantly lower numbers of CD8<sup>+</sup> effector T-cells, with lower expression of activation markers, as well as impaired proliferation and effector function. Using CD8<sup>+</sup> T-cells from a T-cell receptor (TCR) reporter mouse, we verified that this is due to a direct effect of ibrutinib on TCR activity, and demonstrate that co-stimulation via CD28 overcomes these effects. Most interestingly, combination of ibrutinib with blocking antibodies targeting PD-1/PD-L1 axis *in vivo* improved CD8<sup>+</sup> T-cell effector function and control of CLL. In sum, these data emphasize the strong immunomodulatory effects of ibrutinib and the therapeutic potential of its combination with immune checkpoint blockade in CLL.

## **Article summary**

The BTK inhibitor ibrutinib which is used to treat CLL patients is known to impact not only on malignant B-cells, but also to target ITK in T-cells, which might contribute to treatment effects. Here, we show that ibrutinib blocks effector T-cell expansion and function *in vitro* and in a CLL mouse model, which could be amended by combining ibrutinib with PD-1 or PD-L1 antibody treatment.

## Introduction

Within the last decade, a new era of therapeutic opportunities for patients with chronic lymphocytic leukemia (CLL) has begun.(1) Treatment responses, also in patients with relapsed and refractory disease or unfavorable genetic profile, have dramatically improved with the development and approval of kinase inhibitors that target B-cell receptor (BCR) signaling, a well-known driver of disease.(2, 3) Ibrutinib is an orally bioavailable, irreversible inhibitor of Bruton's tyrosine kinase (BTK). Both *in vitro* and in patients, ibrutinib has been shown to potently inhibit B-cell receptor (BCR) signaling, prevent lymphocyte adhesion and homing, and inhibit protective effects of the microenvironment, which yields high response rates and durable remissions in patients with CLL if applied continuously.(4, 5)

In addition to pro-survival pathways in malignant cells, like BCR signaling, T-cells represent an attractive therapeutic target in CLL. T-cells expand along with the disease course in patients and mouse models of CLL.(6, 7) Our recent work has demonstrated a non-redundant role of CD8<sup>+</sup> T-cells in suppressing CLL progression in an IFN $\gamma$ -dependent manner.(8) Yet, chronic exposure to tumor-derived antigens in secondary lymphoid organs leads to their continuous activation, upregulation of inhibitory receptors, such as PD-1, and ultimately exhaustion.(8) Therefore, targeting inhibitory receptors, such as PD-1 and Lag3, offered novel opportunities of therapeutic reactivation of adaptive anti-tumor immunity by immune checkpoint blockade.(9, 10) Notably, immune checkpoint blockade showed promising activity in a subgroup of CLL patients with Richter's transformation, suggesting that unleashing inhibited T-cells results in better control of leukemia progression.(11)

Besides its direct cytotoxic activity against malignant B-cells, ibrutinib also exerts immunomodulatory effects (reviewed by Maharaj et al.).(12) Ibrutinib-mediated inhibition of STAT3 results in decreased expression of immunosuppressive molecules, such as PD-L1 and IL-10, by CLL cells.(13) Gunderson and colleagues have demonstrated that BTK inhibition in tumor-associated myeloid cells reprograms them towards M1-like immunostimulatory phenotypes resulting in enhanced anti-tumoral T-cell activity.(14) In addition to modulating BTK-expressing cells in the microenvironment, ibrutinib has been shown to impact natural killer (NK)- and T-cell activity due to its non-BTK effects on IL-2-inducible T-cell kinase (ITK).(15, 16) In a preclinical study, ITK inhibition by ibrutinib was shown to impair Fc receptor-mediated NK-cell functions and to antagonize cytotoxicity of rituximab.(16) However, NK-cell-mediated cellular cytotoxicity was significantly recovered 12 hours after ibrutinib has been removed, which may be attributed to turnover of ITK.(17) Inhibition of ITK by ibrutinib was further shown to modulate TCR signaling in CD4<sup>+</sup> T-cells and enhance Th1 response *in vitro*.(15) In addition, a reduced number or percentage of regulatory T-cells in peripheral blood of ibrutinib-treated patients was reported.(18, 19) Interestingly, ibrutinib was recently approved for the treatment of refractory chronic graft-versus-host-disease (cGVHD) after allogeneic hematopoietic stem cell transplantation, indicating its potent immunomodulatory effect *in vivo*.(20)

The strong immunomodulatory activity of ibrutinib encouraged several pre-clinical and clinical studies assessing its potential combination with other immunotherapeutic drugs, primarily immune checkpoint blockade.(21) The success of these immunotherapeutic approaches relies on enhancing the functional capacities and proliferation of anti-

tumoral CD8<sup>+</sup> T-cells. Despite a large body of evidence highlighting the immunomodulatory activity of ibrutinib, its exact impact on CD8<sup>+</sup> T-cells in CLL remains less defined. While Long and colleagues observed an increase in CD4<sup>+</sup> and CD8<sup>+</sup> T-cell numbers in ibrutinib-treated patients,(19) a drop in T-cell numbers, activation, and proliferation were reported in another patient cohort.(22) Moreover, it was suggested that ibrutinib can enhance anti-tumoral CD8<sup>+</sup> T-cell function in CLL patients by fostering a switch of T-helper-cell polarization towards anti-tumoral Th1 cells.(15) Yet, this change in Th1 polarization could not be confirmed in a cohort of ibrutinib-treated patients.(19) Thus, in this study we utilized the *Eμ*-TCL1 adoptive transfer (TCL1 AT) model of CLL to monitor CD8<sup>+</sup> T-cell differentiation and function under ibrutinib treatment. Thereby, we observed that this drug reduces the functionality of CD8<sup>+</sup> T-cells which could be overcome by combining ibrutinib with immune checkpoint blockade in the TCL1 AT model. The relevance of these findings for therapeutic applications has to be proven in ongoing clinical trials combining ibrutinib with anti(α)PD-L1 antibody durvalumab for treatment of B-cell lymphoma and CLL patients (<https://clinicaltrials.gov>: NCT02401048 and NCT02733042).

## **Methods**

### **Mouse models**

*Eμ*-TCL1 (TCL1) mice on C57BL/6 background were kindly provided by Dr. Carlo Croce (Ohio State University).(23) C57BL/6 wildtype (WT) mice were purchased from Charles River Laboratories (Sulzfeld, Germany), and Nr4a1<sup>GFP</sup> mice(24) were kindly provided by Dr. Markus Feuerer (DKFZ, Heidelberg).

TCL1 tumor cells of C57BL/6N background were propagated once by adoptive transfer in C57BL/6N mice to ensure having enough tumor cells from the same donor for all treatment arms. Adoptive transfer of TCL1 tumors was performed as previously described.(9, 25) Briefly, 1-2 x 10<sup>7</sup> leukemic TCL1 splenocytes (CD5<sup>+</sup>CD19<sup>+</sup> content of purified cells was typically above 90%) were transplanted by intraperitoneal (i.p.) injection into 2-3 months old C57BL/6N WT females. All animal experiments were carried out according to governmental and institutional guidelines and approved by the local authorities (Regierungspräsidium Karlsruhe, permit numbers: G-36/14, G-123/14, G-16/15, and G-53/15).

### ***In vivo* treatment**

Two to three weeks after tumor cell transplantation, tumor load in blood (defined as the number of CD5<sup>+</sup>CD19<sup>+</sup> CLL cells/ $\mu$ l) was measured, and mice were assigned to different treatment arms to achieve comparable tumor load in all groups at baseline prior to treatment. Ibrutinib (provided by Pharmacyclics LLC, an AbbVie Company) was administered in drinking water containing sterile control vehicle (1% HP- $\beta$ -CD) at a concentration of 0.16 mg/mL, as previously described.(26) For PD-1/PD-L1 blockade,

mice were injected i.p. with 0.2 mg of  $\alpha$ PD-1 (clone: RMP1-14),  $\alpha$ PD-L1 (clone: 10F.9G2), or rat IgG2a isotype control antibody (clone: 2A3; both from BioXcell, West Lebanon, NH) every 3 days for 4 weeks.

### **Flow cytometry and functional assays**

Single cell suspensions from peripheral blood (PB) or lymphoid tissues were prepared and flow cytometric analyses of cell surface proteins and transcription factors were performed as detailed in the supplement and described before.(8, 27) Gating strategies are depicted in the Supplementary Information and antibodies are listed in Supplementary Table 1.

Cytokine release, granzyme B production and degranulation capacity of CD8<sup>+</sup> T-cells were assayed as previously described with minor modifications outlined in the supplement.(9)

Human PB mononuclear cells (PBMCs) or mouse splenocytes were pre-treated for 30 minutes with ibrutinib, CC-292 or ACP-196 (Selleckchem, Munich, Germany), then stimulated with 1  $\mu$ g/ml  $\alpha$ CD3 antibodies (clone HIT3a or 145-2C11, respectively) in 96-well round-bottom microtiter plates at a density of  $2 \times 10^6$ /ml and incubated at 37°C and 5% CO<sub>2</sub> until analyzed by flow cytometry. For assessment of proliferation, cells were stained with 5  $\mu$ M carboxyfluoresceinsuccinimidyl ester (CFSE; eBioscience) prior to drug treatment and stimulation as previously described.(28)

## **Statistical analysis**

Sample size was determined based on expected variance of read-out. No samples or animals were excluded from the analyses. No randomization or blinding was used in animal studies. Data were analysed using Prism 5.04 GraphPad software. Statistical tests of data were one-way ANOVA followed by multiple comparison test or unpaired Student's t-test with Welch approximation to account for unequal variances. When appropriate, paired Student's t-test was used. Values of  $p < 0.05$  were considered to be statistically significant. All graphs show means  $\pm$  SEM, unless otherwise indicated.

## Results

### Ibrutinib modulates effector CD8<sup>+</sup> T-cell differentiation and proliferation in the TCL1 adoptive transfer model

To investigate effects of ibrutinib on CD8<sup>+</sup> T-cells *in vivo*, we utilized the TCL1 AT model of CLL.(9, 25) We transplanted C57BL/6 WT mice with TCL1 splenocytes, and after 2 weeks mice were assigned to treatment with ibrutinib or vehicle according to tumor load in PB. In line with published data,(29) ibrutinib treatment resulted in a significant decrease in CLL development in comparison to vehicle-treated mice, as evident by a decrease in CD5<sup>+</sup>CD19<sup>+</sup> cell counts in PB and decreased splenomegaly and hepatomegaly (Figure 1A-B). Moreover, CLL cell proliferation was significantly reduced, as measured by Ki-67 staining (Figure 1C), confirming efficient cytotoxic activity of the drug.

We then evaluated the effect of ibrutinib on anti-tumoral CD8<sup>+</sup> T-cells. We have recently shown that CLL development in TCL1 mice induces the differentiation of an anti-tumoral, oligoclonal effector CD8<sup>+</sup> T-cell population that controls tumor development in an IFN $\gamma$ -dependent manner.(8) Accordingly, we analyzed the splenic CD8<sup>+</sup> T-cell composition using CD44 and CD127, which divide CD8<sup>+</sup> T-cells into CD127<sup>hi</sup>CD44<sup>low</sup> naïve, CD127<sup>hi</sup>CD44<sup>hi</sup> memory, and CD127<sup>low</sup>CD44<sup>int-hi</sup> effector subsets (Figure 1D). As expected, CLL development induced a sizable expansion of CD127<sup>low</sup>CD44<sup>+</sup> effector T-cells in vehicle-treated mice in comparison to untransplanted WT controls (Figure 1D-E). Of interest, the percentage and absolute numbers of the effector population were lower in ibrutinib-treated mice (Figure 1D-E). This was accompanied by decreased expression of activation markers like CD69 and CD137 on CD8<sup>+</sup> T-cells (Figure 1F),

and decreased expression of transcription factors that regulate effector T-cell differentiation, such as T-box transcription factor T-bet and Eomesodermin (Eomes) (Figure 1G).<sup>(30)</sup> Furthermore, CD8<sup>+</sup> T-cell proliferation was significantly lower in ibrutinib- compared to vehicle-treated TCL1 mice, reaching levels similar to non-tumor control mice (Figure 1H). The drop in effector population, activation markers and proliferation of CD8<sup>+</sup> T-cells was also observed when treatment started at later stages of disease when all mice had more than 5,000 CLL cells/  $\mu$ l of blood, the leukemic threshold in CLL patients (Suppl. Figure 1A).

We next examined whether the observed changes in CD8<sup>+</sup> T-cells are caused by a direct impact of ibrutinib on these cells or rather reflect a secondary normalization of the T-cell compartment due to the decrease in tumor load. Thus, we analyzed CD8<sup>+</sup> T-cells in vehicle- and ibrutinib-treated mice having a similar disease load, as measured by CLL cell infiltration in spleen and liver. While the vehicle-treated mice showed signs of overt leukemia with severe hepato-splenomegaly after 3 weeks of starting the treatment, ibrutinib successfully suppressed CLL development during that time. Nonetheless, mice continuously receiving ibrutinib succumbed to full-blown leukemia at week 4 post treatment exhibiting similar disease load to vehicle group at week 3 (Suppl. Figure 1B). Analysis of the spleen CD8<sup>+</sup> T-cell compartment of end-stage vehicle or ibrutinib-treated mice with comparable tumor load revealed a decrease in effector T-cell percentage and numbers, accompanied by a significant drop in activation marker expression and proliferation in the latter group (Suppl. Figure 1C-E). This suggests that the observed differences in CD8<sup>+</sup> T-cells in ibrutinib- vs vehicle-treated mice were not secondary to changes in tumor load.

### **Ibrutinib modulates CD8<sup>+</sup> T-cell function in the TCL1 adoptive transfer model**

We next examined the impact of ibrutinib treatment on the expression of inhibitory receptors like PD-1, CD244 and Lag3 on CD8<sup>+</sup> T-cells. We observed a substantial drop in the expression of these markers in the ibrutinib cohort (Figure 2A). As T-cell inhibitory receptors are mainly induced upon activation of tumor-reactive T-cells,(31) we evaluated whether the drop in their expression reflects an improvement in T-cell function or is rather a consequence of the drop in T-cell activation in ibrutinib-treated mice (Figure 1F). Thus, we analyzed the functional capacities of CD8<sup>+</sup> T-cells using intracellular flow cytometric staining following mitogen PMA/ionomycin stimulation. CD8<sup>+</sup> T-cells from ibrutinib-treated mice exhibited lower degranulation potential, as measured by CD107a presentation on the cell surface (Figure 2B). Furthermore, granzyme A (GzmA) and GzmB expression in CD8<sup>+</sup> T-cell significantly dropped in these mice (Figure 2C). Moreover, production of IFN $\gamma$  was significantly lower in CD8<sup>+</sup> T-cells from ibrutinib-treated mice (Figure 2D), collectively indicating poor cytotoxic and effector function of these cells. The changes in cytokine production and cytolytic abilities were primarily attributed to the decrease in the effector CD8<sup>+</sup> fraction after ibrutinib treatment. Nonetheless, degranulation capacity, GzmA and GzmB levels were also decreased when focusing the analysis on the minor effector or PD-1<sup>+</sup> population in ibrutinib-treated mice (Suppl. Figure 2A-F). In sum, these data indicate that *in vivo* ibrutinib treatment alters activation, effector differentiation and function of CD8<sup>+</sup> T-cells in the TCL1 AT model.

### **Ibrutinib modulates T-cell receptor signaling in CD8<sup>+</sup> T-cells *in vitro***

We then investigated the mechanisms that control the above-mentioned changes in T-cell function. While ibrutinib can indirectly impact T-cells through BTK inhibition in CLL cells or other antigen presenting cells in the microenvironment, the drug can potentially affect T-cell function in a direct manner through its off-target effects on ITK. To examine these possibilities, we tested the effect of different BTK inhibitors on TCR signaling using a reporter mouse line for *Nr4a1*, an immediate target of TCR activation.(24) Splenocytes from *Nr4a1*-GFP mice were pre-treated with ibrutinib or DMSO as control and then stimulated with  $\alpha$ CD3 for 6 hours. We primarily used ibrutinib in a dose range of 100-1,000 nM, which results in ITK occupancy of up to 50% corresponding to the level observed *in vivo* in ibrutinib-treated CLL patients.(15)  $\alpha$ CD3 stimulation resulted in a rapid increase of the *Nr4a1*-GFP signal in CD8<sup>+</sup> T-cells in DMSO controls (Figure 3A). Interestingly, ibrutinib treatment resulted in a 15% decrease in the *Nr4a1*-GFP MFI at 100 nM and abrogation of *Nr4a1*-GFP induction in most of the cells at a concentration of 1  $\mu$ M (Figure 3A). Similarly, the induction of early activation marker CD69 was significantly reduced at a concentration of 100 nM or higher (Figure 3A). We compared these effects to the more specific BTK inhibitors, CC-292 and ACP-196, which have ITK IC<sub>50</sub> values of 24 and 1,000 nM, respectively, compared to that of 4.9 nM of ibrutinib.(32) Interestingly, we observed that the decrease in *Nr4a1*-GFP and CD69 signals was less pronounced in CC-292 and was entirely absent upon ACP-196 treatment (Figure 3A), indicating that these effects are BTK-independent. In line with these results, ibrutinib, but not ACP-196 treatment of mouse splenocytes inhibited the expression of other activation markers like CD25, CD44 and CD137 on CD8<sup>+</sup> T-cells in

response to  $\alpha$ CD3 stimulation (Figure 3B, Suppl. Figure 3A-C). In addition, CFSE dilution assays showed that ibrutinib, but not ACP-196, inhibited CD8<sup>+</sup> T-cell proliferation (Suppl. Figure 3D). Similar to murine splenocytes, treatment of human PMBCs with ibrutinib resulted in a dose-dependent decrease in proliferation of CD8<sup>+</sup> T-cells in response to  $\alpha$ CD3 stimulation (Figure 3C). Collectively, these data suggest that ibrutinib can modulate CD8<sup>+</sup> T-cell response to TCR stimulation in a BTK-independent manner.

### **Strong co-stimulatory signals can rescue CD8<sup>+</sup> T-cells from inhibitory effects of ibrutinib *in vitro***

We next evaluated potential approaches to unleash CD8<sup>+</sup> T-cells from ibrutinib's inhibitory effects. Previous work has shown that CD28 signaling is intact in the absence of ITK.(33) Thus, we hypothesized that strong CD28 co-stimulation can hijack ibrutinib inhibitory effects on CD8<sup>+</sup> T-cells. Therefore, we evaluated the effect of the drug on murine CD8<sup>+</sup> T-cells stimulated with  $\alpha$ CD3 alone or  $\alpha$ CD3 plus  $\alpha$ CD28. The addition of  $\alpha$ CD28 antibody had no impact on the drop of *Nr4a1*-GFP signal after ibrutinib treatment (Figure 4A), which goes in line with previous work demonstrating that *Nr4a1* induction by TCR stimulation is independent of CD28 co-stimulation and remains intact in *Cd28*<sup>-/-</sup> mice.(24) Interestingly, CD28 co-stimulation completely abolished the inhibition of activation marker expression that is caused by ibrutinib (Figure 4A). Moreover, CD8<sup>+</sup> T-cell proliferation was rescued to normal levels when co-stimulated by  $\alpha$ CD28 (Figure 4B). Similar results were observed by addition of  $\alpha$ CD28 antibody to

human CD8<sup>+</sup> T-cells (Figure 4C), confirming that strong co-stimulatory signals can circumvent the TCR inhibitory effects of ibrutinib.

### **Blocking PD-1/PD-L1 axis enhances the anti-leukemic activity of ibrutinib**

In the subsequent experiments we investigated possible immunomodulatory drugs that can recapitulate the *in vitro* effects of  $\alpha$ CD28 antibodies and thereby reverse the block of CD8<sup>+</sup> T-cell differentiation in the TCL1 AT model. In light of recent results showing CD28 signaling as the primary target of PD-1 blockade,(34, 35) we reasoned that blocking PD-1/PD-L1 axis can enhance anti-tumoral T-cell activity and improve therapeutic efficacy of ibrutinib. Thus, we treated CLL-bearing mice with ibrutinib alone or in combination with  $\alpha$ PD-1 or  $\alpha$ PD-L1 antibodies. As shown in Suppl. Figure 4, all treatment groups had comparable tumor load at the start of the treatment. Consistent with our previous work, blocking PD-1/PD-L1 axis by  $\alpha$ PD-L1 resulted in delayed CLL development in PB, spleen and bone marrow (BM) (Figure 5A-C). The effects were more pronounced for  $\alpha$ PD-L1 compared to  $\alpha$ PD-1 treatment, which is likely due to the additional effects of  $\alpha$ PD-L1 antibodies on tumor-associated myeloid cells, as shown by us and others.(9, 36) Interestingly, combination of ibrutinib with PD-1 or PD-L1 blocking antibodies resulted in enhanced disease control in PB, spleen and BM, which was most pronounced in the  $\alpha$ PD-L1/ibrutinib combination (Figure 5A-C), confirming a therapeutic efficacy of this combination.

### **Blocking PD-1/PD-L1 axis expands the effector population and enhances the functional capacity of CD8<sup>+</sup> T-cells**

We then examined the effect of PD-1/PD-L1 combination with ibrutinib on CD8<sup>+</sup> T-cell activity. We restricted our analysis to αPD-1 plus ibrutinib treatment as these mice had more comparable tumor load to the ibrutinib single arm (Figure 5A-C), and thereby we could exclude changes in T-cells that are caused by differences in disease load. In line with our previous data, ibrutinib reduced the percentage of effector population, and decreased activation, proliferation and functional capacities of CD8<sup>+</sup> T-cells (Figure 6A-D). Interestingly, combination of ibrutinib with αPD-1 resulted in a significant increase in effector CD8<sup>+</sup> T-cell percentages (Figure 6A), which was accompanied by an increase in activation marker expression on CD8<sup>+</sup> T-cells (Figure 6B). Moreover, CD8<sup>+</sup> T-cell functional capacity was improved by the combination treatment, as shown by a significant increase in degranulation capacity and IFN $\gamma$  production (Figure 6C-D). The increase in degranulation capacity and IFN $\gamma$  production was also observed when focusing the analysis on the CD8<sup>+</sup> effector T-cell population (Suppl. Figure 5A-B). Collectively, these data show that blocking PD-1/PD-L1 pathway can improve CD8<sup>+</sup> T-cell function and enhance CLL control after ibrutinib treatment.

## Discussion

Ibrutinib is approved as successful inhibitor of BTK for treatment of CLL and other B-cell lymphomas. In addition, it is also the first clinically available inhibitor of ITK.(15) ITK is expressed in T-cells in which it is, as a major player in TCR signaling, responsible for calcium mobilization, cytoskeleton reorganization, synapse formation and adhesion.(37) Deletion or inhibition of ITK in CD8<sup>+</sup> T-cells results in their decreased expansion, delayed expression of cytolytic effector molecules, and defective degranulation upon TCR activation.(38) This leads to a global defect in the cytolysis of pathogens, and as a consequence, to reduced viral clearance. In line with this, dramatic *in vivo* immunomodulation by ibrutinib has led to its approval for the treatment of refractory cGVHD,(20) but the mechanisms underlying this clinical efficacy are poorly understood. So far, modulating effects of ibrutinib on the differentiation of CD4<sup>+</sup> T-cells, like Th1, Th2, Th17 and Treg cells, were described.(15, 19, 22) In the current study, we observed a negative impact of ibrutinib on CD8<sup>+</sup> T-cell proliferation and function in the TCL1 AT model, which reduces their phenotype to a level of tumor naïve control mice. As our *in vitro* data confirmed CD8<sup>+</sup> T-cell inhibition by ibrutinib, but not the specific BTK inhibitor ACP-196, this effect is BTK-independent and most likely mediated by inhibition of ITK downstream of the TCR. Along this line, CC-292, an inhibitor with a higher selectivity for BTK, had a lower impact on T-cell activity *in vitro*, and has been previously shown not to impair T-cell function in the TCL1 AT model.(39) But as these drugs might have different efficacies in patients, extrapolating clinical effects from these pre-clinical observations has to be done with caution. Our observations in the TCL1 AT model seem to be in contrast to published data describing an increase of CD8<sup>+</sup> T-cell numbers and their

reduced expression of inhibitory receptors, like PD-1, in CLL patients after 8 to 20 weeks of treatment with ibrutinib.(19) The results of this study suggest that this may be due to diminished activation-induced cell death of T-cells through ITK inhibition. As our data demonstrate that inhibition of ITK by ibrutinib decreases TCR signaling and thereby activation of T-cells, a consequence of that is not only reduced functional properties, as we show, but also diminished activation-induced cell death, confirming what was observed by Long et al. in CLL patients.(19) A further study documented that ibrutinib decreases CD8 T-cell proliferation and activation in patients 8 weeks after treatment start.(22) Yet, these results have been largely viewed as a sign of favourable immune normalization under ibrutinib treatment, rather than a direct side effect of the drug. In light of our *in vitro* and *in vivo* results, it is more likely that these findings in CLL patients are due to the off-target effects of ibrutinib on ITK. In a further study that investigated T-cells in CLL patients before and after one year of treatment with ibrutinib, disease-associated, elevated T-cell numbers and T-cell-related cytokine levels in PB had normalized, and T-cell repertoire diversity had increased significantly in treated patients.(40) Considering the broad effects of BTK blockade on functional properties of many immune cell types, these changes in the T-cell compartment might be due to ibrutinib's ability to rewire the carefully constructed, supportive microenvironmental network in CLL, which presumably contributes to the therapeutic success of this drug.(41) But as ibrutinib, first-of-all, considerably redistributes malignant B-cells from lymph nodes to blood which ultimately results in a reduction of tumor burden, this suggests that normalization of the T-cell compartment under ibrutinib treatment is secondary to the effect of the drug on CLL cell numbers and their localization. This is

supported by our previous results as well as published data of others showing that T-cell expansion and exhaustion positively correlates with tumor load and is predominantly happening in secondary lymphoid organs.(7-9) Along this line, enhanced engraftment and efficacy of CLL patient-derived chimeric antigen receptor (CAR) T-cells after more than 1 year of treatment with ibrutinib can be also explained by a normalization of T-cells associated with a reduction of exhaustion phenotype, secondary to the effective control of CLL by the drug.(42) In this study, the authors further show that *ex vivo* treatment of CLL CAR T-cells with ibrutinib does not impact on their proliferation or function. Our data now clearly show that this observation is due to a commonly used stimulation protocol for T-cells *in vitro* in which  $\alpha$ CD3 and  $\alpha$ CD28 antibodies are combined as stimuli. Co-stimulation of CD8<sup>+</sup> T-cells with  $\alpha$ CD28 was also used by Dubovsky et al. who describe that ibrutinib does not affect TCR signaling and function of these cells.(15) This observation was in contrast to results obtained in ITK-deficient mice which show impaired TCR-dependent signaling and CD8<sup>+</sup> T-cell effector function in response to viral infections.(43) We now show that inhibition of T-cell activity by ibrutinib can be overcome by co-stimulatory signaling mediated by CD28, which is known to be independent of ITK.(33) In line with our findings, stimulation of ITK-deficient CD8<sup>+</sup> T-cells with  $\alpha$ CD3 only leads to impaired expansion and activity.(43)

Considering our observations that ibrutinib negatively impacts on the activity of CD8<sup>+</sup> T-cells, one needs to investigate whether patients under long-term ibrutinib treatment have reduced adaptive immunity. In early clinical studies and applications of ibrutinib, this was hard to assess, as treated patients were relapsed and refractory, as well as high-risk CLL who have a profound immune suppression and perturbation of both innate

and adaptive immunity, and therefore an increased susceptibility to infections is likely to be caused by the disease.(44) Only more recently, with the approval of ibrutinib as first-line therapy for CLL, high rates of infectious complications in patients on ibrutinib monotherapy and in combination with other drugs are observed.(45) However, in comparison to the severe effects chemotherapy has on the immune system of patients, ibrutinib is reasonably tolerated, and by monitoring the impact of ibrutinib on patients' immune status, or by preventing immunosuppressive adverse effects by rational combination treatment approaches with drugs that improve T-cell effector function, outcome for patients can be even further improved. Recent data of clinical trials with the highly selective BTK inhibitor acalabrutinib showed overall response rates of 85% in treatment naïve CLL patients and 94% in relapsed/refractory cases.(46, 47) Most adverse events (AEs) observed in these trials were mild or moderate (grade 1-2) and were most commonly diarrhea and headache. It was hypothesized that due to its greater selectivity for BTK, acalabrutinib has favourable pharmacokinetic properties and improved toxicity profile than ibrutinib. Considering however the short history of acalabrutinib treatment compared to ibrutinib and the lack of a head-to-head comparison of the two drugs in CLL patients, it remains unclear whether the long-term immune side effects of the drugs are comparable.

Of interest, the immunomodulatory effect of ibrutinib can be even of therapeutic advantage as shown in patients with relapsed CLL after allogeneic hematopoietic stem cell transplantation, in which ibrutinib was tolerable and effective.(48)

Our data in the TCL1 AT model show that combining ibrutinib with immune checkpoint blockade leads to enhanced CD8<sup>+</sup> T-cell function and reduced CLL progression. Both

$\alpha$ PD-1 and  $\alpha$ PD-L1 treatment improved the therapeutic effect of ibrutinib, with better results observed with  $\alpha$ PD-L1. As PD-L1 is expressed by CLL and myeloid cells in this model,(25) this antibody has a broader activity compared to  $\alpha$ PD-1. Besides blocking the interaction with PD-1,  $\alpha$ PD-L1, but not  $\alpha$ PD-1 antibodies, were shown to modulate myeloid cell subsets within the tumor microenvironment via activating Fc $\gamma$  receptors.(36) Furthermore, blocking PD-L1 directly on tumor cells dampens their glycolysis, leaving more available glucose in the extracellular tumor milieu for T-cells, which enhances their activity.(49)

Testing the combination of ibrutinib with immune checkpoint blockade in the mouse model allowed us to monitor tumor load in all organs affected by disease. In line with observations in CLL patients, ibrutinib as single-agent was not able to reduce malignant cells in the BM, which explains why patients and mice relapse if therapy is discontinued. Interestingly, if combined with  $\alpha$ PD-1 or  $\alpha$ PD-L1, tumor control in the BM was as efficient as in spleen and blood, suggesting that the combination of ibrutinib with checkpoint blockade might be able to eradicate CLL cells more efficiently leading eventually to a cure of patients.

## **Acknowledgements**

This study was supported by the German José Carreras Foundation (R14/23), the German Cancer Aid (grant number 112069), the BMBF-Network “PRECiSe” (031L0076A), the ERA-NET TRANSCAN-2 program JTC 2014–project FIRE-CLL, and the Cooperation Program in Cancer Research of the DKFZ and Israel’s Ministry of Science, Technology and Space. St. St. was supported by the DFG (SFB1074 subproject B1).

## **Authorship Contributions**

BSH designed the study, performed experiments, analyzed and interpreted data, prepared figures, and wrote the manuscript. HY, YD, PMR and RS performed experiments, analyzed and interpreted data. StSt and PL critically advised the study and reviewed the manuscript. MS designed and supervised the study, interpreted data, and wrote the manuscript.

## **Disclosure of Conflicts of Interest**

The authors have declared that they have no competing interests.

## References

1. Burger JA, O'Brien S. Evolution of CLL treatment — from chemoimmunotherapy to targeted and individualized therapy. *Nat Rev Clin Oncol*. 2018;15(8):510-527.
2. Wiestner A. The role of B-cell receptor inhibitors in the treatment of patients with chronic lymphocytic leukemia. *Haematologica*. 2015;100(12):1495-1507.
3. Farooqui MZH, Valdez J, Martyr S, et al. Ibrutinib for previously untreated and relapsed or refractory chronic lymphocytic leukaemia with TP53 aberrations: a phase 2, single-arm trial. *Lancet Oncol*. 2015;16(2):169-176.
4. Badar T, Burger JA, Wierda WG, O'Brien S. Ibrutinib: a paradigm shift in management of CLL. *Exp Rev Hematol*. 2014;7(6):705-717.
5. Davids MS, Brown JR. Ibrutinib: a first in class covalent inhibitor of Bruton's tyrosine kinase. *Future Oncol*. 2014;10(6):957-967.
6. Hofbauer JP, Heyder C, Denk U, et al. Development of CLL in the TCL1 transgenic mouse model is associated with severe skewing of the T-cell compartment homologous to human CLL. *Leukemia*. 2011;25(9):1452-1458.
7. Riches JC, Davies JK, McClanahan F, et al. T cells from CLL patients exhibit features of T-cell exhaustion but retain capacity for cytokine production. *Blood*. 2013;121(9):1612-1621.
8. Hanna BS, Roessner PM, Yazdanparast H, et al. Control of chronic lymphocytic leukemia development by clonally-expanded CD8+ T-cells that undergo functional exhaustion in secondary lymphoid tissues. *Leukemia*. 2019;33(3):625-637.
9. McClanahan F, Hanna B, Miller S, et al. PD-L1 Checkpoint Blockade Prevents Immune Dysfunction and Leukemia Development in a Mouse Model of Chronic Lymphocytic Leukemia. *Blood*. 2015;126(2):203-211.
10. Wierz M, Pierson S, Guyonnet L, et al. Dual PD1/LAG3 immune checkpoint blockade limits tumor development in a murine model of chronic lymphocytic leukemia. *Blood*. 2018;131(14):1617-1621.
11. Ding W, LaPlant BR, Call TG, et al. Pembrolizumab in patients with CLL and Richter transformation or with relapsed CLL. *Blood*. 2017;129(26):3419-3427.
12. Maharaj K, Sahakian E, Pinilla-Ibarz J. Emerging role of BCR signaling inhibitors in immunomodulation of chronic lymphocytic leukemia. *Blood Adv*. 2017;1(21):1867-1875.
13. Kondo K, Shaim H, Thompson PA, et al. Ibrutinib modulates the immunosuppressive CLL microenvironment through STAT3-mediated suppression of regulatory B-cell function and inhibition of the PD-1/PD-L1 pathway. *Leukemia*. 2018;32(4):960-970.
14. Gunderson AJ, Kaneda MM, Tsujikawa T, et al. Bruton Tyrosine Kinase-Dependent Immune Cell Cross-talk Drives Pancreas Cancer. *Cancer Discov*. 2016;6(3):270-285.
15. Dubovsky JA, Beckwith KA, Natarajan G, et al. Ibrutinib is an irreversible molecular inhibitor of ITK driving a Th1-selective pressure in T lymphocytes. *Blood*. 2013;122(15):2539-2549.
16. Kohrt HE, Sagiv-Barfi I, Rafiq S, et al. Ibrutinib antagonizes rituximab-dependent NK cell-mediated cytotoxicity. *Blood*. 2014;123(12):1957-1960.
17. Ng PP, Lu DK, Sukbuntherng J, et al. Ibrutinib Enhances the Activity of Anti-CD20 Antibodies in an MCL Mouse Model: Effect of Drug at Clinically Relevant Concentrations on ADCC and ADCP. *Blood*. 2015;126(23):3998-3998.
18. Podhorecka M, Goracy A, Szymczyk A, et al. Changes in T-cell subpopulations and cytokine network during early period of ibrutinib therapy in chronic lymphocytic leukemia patients: the significant decrease in T regulatory cells number. *Oncotarget*. 2017;8(21):34661-34669.
19. Long M, Beckwith K, Do P, et al. Ibrutinib treatment improves T cell number and function in CLL patients. *J Clin Invest*. 2017;127(8):3052-3064.

20. Miklos D, Cutler CS, Arora M, et al. Ibrutinib for chronic graft-versus-host disease after failure of prior therapy. *Blood*. 2017;130(21):2243-2250.
21. Sagiv-Barfi I, Kohrt HE, Czerwinski DK, et al. Therapeutic antitumor immunity by checkpoint blockade is enhanced by ibrutinib, an inhibitor of both BTK and ITK. *Proc Natl Acad Sci U S A*. 2015;112(9):E966-972.
22. Niemann CU, Herman SEM, Maric I, et al. Disruption of in vivo Chronic Lymphocytic Leukemia Tumor–Microenvironment Interactions by Ibrutinib – Findings from an Investigator-Initiated Phase II Study. *Clin Cancer Res*. 2016;22(7):1572-1582.
23. Bichi R, Shinton SA, Martin ES, et al. Human chronic lymphocytic leukemia modeled in mouse by targeted TCL1 expression. *Proc Natl Acad Sci U S A*. 2002;99(10):6955-6960.
24. Moran AE, Holzapfel KL, Xing Y, et al. T cell receptor signal strength in Treg and iNKT cell development demonstrated by a novel fluorescent reporter mouse. *J Exp Med*. 2011;208(6):1279-1289.
25. Hanna BS, McClanahan F, Yazdanparast H, et al. Depletion of CLL-associated patrolling monocytes and macrophages controls disease development and repairs immune dysfunction in vivo. *Leukemia*. 2016;30(3):570-579.
26. Chang BY, Huang MM, Francesco M, et al. The Bruton tyrosine kinase inhibitor PCI-32765 ameliorates autoimmune arthritis by inhibition of multiple effector cells. *Arthritis Res Ther*. 2011;13(4):R115.
27. Haderk F, Schulz R, Iskar M, et al. Tumor-derived exosomes modulate PD-L1 expression in monocytes. *Sci Immunol*. 2017;2(13).
28. Quah BJ, Warren HS, Parish CR. Monitoring lymphocyte proliferation in vitro and in vivo with the intracellular fluorescent dye carboxyfluorescein diacetate succinimidyl ester. *Nat Protoc*. 2007;2(9):2049-2056.
29. Ponader S, Chen SS, Buggy JJ, et al. The Bruton tyrosine kinase inhibitor PCI-32765 thwarts chronic lymphocytic leukemia cell survival and tissue homing in vitro and in vivo. *Blood*. 2012;119(5):1182-1189.
30. Kaech SM, Cui W. Transcriptional control of effector and memory CD8+ T cell differentiation. *Nat Rev Immunol*. 2012;12(11):749-761.
31. Fuertes Marraco SA, Neubert NJ, Verdeil G, Speiser DE. Inhibitory Receptors Beyond T Cell Exhaustion. *Front Immunol*. 2015;6:310.
32. Barf T, Covey T, Izumi R, et al. Acalabrutinib (ACP-196): A Covalent Bruton Tyrosine Kinase Inhibitor with a Differentiated Selectivity and In Vivo Potency Profile. *J Pharmacol Exp Ther*. 2017;363(2):240-252.
33. Li C-R, Berg LJ. Cutting Edge: Itk Is Not Essential for CD28 Signaling in Naive T Cells. *J Immunol*. 2005;174(8):4475-4479.
34. Kamphorst AO, Wieland A, Nasti T, et al. Rescue of exhausted CD8 T cells by PD-1-targeted therapies is CD28-dependent. *Science*. 2017;355(6332):1423-1427.
35. Hui E, Cheung J, Zhu J, et al. T cell costimulatory receptor CD28 is a primary target for PD-1-mediated inhibition. *Science*. 2017;355(6332):1428-1433.
36. Dahan R, Segal E, Engelhardt J, et al. FcγRs Modulate the Anti-tumor Activity of Antibodies Targeting the PD-1/PD-L1 Axis. *Cancer Cell*. 2015;28(3):285-295.
37. Bunnell SC, Diehn M, Yaffe MB, et al. Biochemical Interactions Integrating Itk with the T Cell Receptor-initiated Signaling Cascade. *J Biol Chem*. 2000;275(3):2219-2230.
38. Kapnick SM, Stinchcombe JC, Griffiths GM, Schwartzberg PL. Inducible T Cell Kinase Regulates the Acquisition of Cytolytic Capacity and Degranulation in CD8<sup>+</sup> CTLs. *J Immunol*. 2017;198(7):2699-2711.

39. Lee-Vergés E, Hanna BS, Yazdanparast H, et al. Selective BTK inhibition improves bendamustine therapy response and normalizes immune effector functions in chronic lymphocytic leukemia. *Int J Cancer*. 2019;144(11):2762-2773.
40. Yin Q, Sivina M, Robins H, et al. Ibrutinib Therapy Increases T Cell Repertoire Diversity in Patients with Chronic Lymphocytic Leukemia. *J Immunol*. 2017;198(4):1740-1747.
41. Bachireddy P, Wu CJ. Arresting the Inflammatory Drive of Chronic Lymphocytic Leukemia with Ibrutinib. *Clin Cancer Res*. 2016;22(7):1547-1549.
42. Fraietta JA, Beckwith KA, Patel PR, et al. Ibrutinib enhances chimeric antigen receptor T-cell engraftment and efficacy in leukemia. *Blood*. 2016;127(9):1117-1127.
43. Atherly LO, Brehm MA, Welsh RM, Berg LJ. Tec Kinases Itk and Rlk Are Required for CD8<sup>+</sup> T Cell Responses to Virus Infection Independent of Their Role in CD4<sup>+</sup> T Cell Help. *J Immunol*. 2006;176(3):1571-1581.
44. Kipps TJ, Stevenson FK, Wu CJ, et al. Chronic lymphocytic leukaemia. *Nat Rev Dis Primers*. 2017;3:16096.
45. Tillman BF, Pauff JM, Satyanarayana G, Talbott M, Warner JL. Systematic review of infectious events with the Bruton tyrosine kinase inhibitor ibrutinib in the treatment of hematologic malignancies. *Eur J Haematol*. 2018;100(4):325-334.
46. Sharman JP, Banerji V, Fogliatto LM, et al. ELEVATE TN: Phase 3 Study of Acalabrutinib Combined with Obinutuzumab (O) or Alone Vs O Plus Chlorambucil (Clb) in Patients (Pts) with Treatment-Naive Chronic Lymphocytic Leukemia (CLL). *Blood*. 2019;134(Supplement\_1):31.
47. Byrd JC, Wierda WG, Schuh A, et al. Acalabrutinib monotherapy in patients with relapsed/refractory chronic lymphocytic leukemia: updated phase 2 results. *Blood*. 2019 Dec 26. [Epub ahead of print]
48. Ryan CE, Sahaf B, Logan AC, et al. Ibrutinib efficacy and tolerability in patients with relapsed chronic lymphocytic leukemia following allogeneic HCT. *Blood*. 2016;128(25):2899-2908.
49. Chang C-H, Qiu J, O'Sullivan D, et al. Metabolic Competition in the Tumor Microenvironment Is a Driver of Cancer Progression. *Cell*. 2015;162(6):1229-1241.

## Figure legends

### Figure 1: Ibrutinib modulates effector CD8<sup>+</sup> T-cell differentiation and proliferation in the TCL1 adoptive transfer model

C57BL/6 mice were transplanted with splenocytes from leukemic TCL1 mice, and after two weeks assigned to treatment with ibrutinib (0.16 mg/mL) or vehicle control in drinking water. Mice were sacrificed after 2 weeks of treatment. Untransplanted C57BL/6 mice (n=3) were used as controls. **A)** Absolute numbers of CD5<sup>+</sup>CD19<sup>+</sup> CLL cells in peripheral blood analyzed by flow cytometry, and **B)** spleen and liver weight of vehicle- or ibrutinib-treated mice (n=4). **C)** Flow cytometric analysis of Ki-67 expression in CD5<sup>+</sup>CD19<sup>+</sup> CLL cells in spleen from of vehicle- or ibrutinib-treated mice (n=4). **D)** Flow cytometric analysis of splenic CD3<sup>+</sup>CD8<sup>+</sup> T-cells from vehicle- or ibrutinib-treated mice (n=4). Cell subsets were defined as naïve (CD127<sup>hi</sup>CD44<sup>low</sup>), memory (Mem; CD127<sup>hi</sup>CD44<sup>hi</sup>) and effector (Eff; CD127<sup>low</sup>CD44<sup>int-hi</sup>) cells. **E)** Absolute numbers of splenic CD8<sup>+</sup> effector cells from control, vehicle- or ibrutinib-treated mice (n=4). **F)** Flow cytometric analysis of CD69 and CD137, **G)** T-bet and Eomes, and **H)** Ki-67 expression on CD8<sup>+</sup> T-cells from control, vehicle- or ibrutinib-treated mice (n=4).

Results are representative of at least 2 independent experiments. Graphs show means ± SEM. \*\*p<0.01, \*\*\*p<0.001

### Figure 2: Ibrutinib modulates CD8<sup>+</sup> T-cell function in the TCL1 adoptive transfer model

C57BL/6 mice were transplanted with splenocytes from leukemic TCL1 mice, and after two weeks assigned to treatment with ibrutinib (0.16 mg/mL) or vehicle control in

drinking water. Mice were sacrificed after 2 weeks of treatment. **A)** Flow cytometric analysis of PD-1, CD244 and Lag3 expression on CD8<sup>+</sup> T-cells from vehicle- or ibrutinib-treated mice (n=4). **B-D)** Cytotoxic function of CD8<sup>+</sup> T-cells was assessed by flow cytometric analysis of **B)** degranulation capacity, as measured by CD107a expression on the cell surface, **C)** GzmA and GzmB expression, or **D)** IFN $\gamma$  production (n=4).

Graphs show means  $\pm$  SEM. \*p<0.05, \*\*p<0.01, \*\*\*p<0.001; nMFI = normalized median fluorescence intensity

**Figure 3: Ibrutinib modulates T-cell receptor signaling in CD8<sup>+</sup> T-cells *in vitro***

**A)** Splenocytes from *Nr4a1*<sup>GFP</sup> transgenic mice (n=3) were pretreated with different concentrations of ibrutinib, ACP-196, CC-292 or DMSO for 30 minutes, and then stimulated with  $\alpha$ CD3 antibody for 6 hours. *Nr4a1*-GFP (left panels), and CD69 (right panels) expression was analyzed by flow cytometry in viable, 7-aminoactinomycin D (7-AAD)-negative, single CD8<sup>+</sup> T-cells. The relative percentages of *Nr4a1*-GFP- or CD69-positive cells are depicted on the right. **B)** Splenocytes from C57BL/6 mice (n=3) were pretreated with different concentrations of ibrutinib or DMSO for 30 minutes and then stimulated with  $\alpha$ CD3 antibody. CD25, CD44 and CD137 expression was analyzed by flow cytometry in viable, 7-AAD-negative, single CD8<sup>+</sup> T-cells after 24 hours. **C)** PBMCs from healthy donors (n=5) were labeled with 5  $\mu$ M CFSE, pretreated with different concentrations of ibrutinib or DMSO for 30 minutes and then stimulated with  $\alpha$ CD3 antibody. Proliferation as measured by CFSE dilution after 72 hours was analyzed by flow cytometry in viable, 7-AAD-negative, single CD8<sup>+</sup> T-cells.

Graphs show means  $\pm$  SEM. \* $p < 0.05$ , \*\* $p < 0.01$ , \*\*\* $p < 0.001$ ; MFI = median fluorescence intensity

**Figure 4: Strong co-stimulatory signals can rescue CD8<sup>+</sup> T-cells from inhibitory effects of ibrutinib *in vitro***

**A)** Left panel: splenocytes from *Nr4a1*<sup>GFP</sup> transgenic mice (n=3) were pretreated with different concentrations of ibrutinib or DMSO for 30 minutes, and then stimulated with either  $\alpha$ CD3 or  $\alpha$ CD3 plus  $\alpha$ CD28 antibodies for 6 hours. *Nr4a1*-GFP, expression was analyzed by flow cytometry in viable, 7-aminoactinomycin D (7-AAD)-negative, single CD8<sup>+</sup> T-cells. Middle and right panel: splenocytes from C57BL/6 mice (n=4) were pretreated with different concentrations of ibrutinib or DMSO for 30 minutes and then stimulated with either  $\alpha$ CD3 or  $\alpha$ CD3 plus  $\alpha$ CD28 antibodies. CD25, and CD44 expression were analyzed by flow cytometry in CD8<sup>+</sup> T-cells after 24 hours. **B)** Splenocytes from C57BL/6 mice (n=4) were labeled with CFSE, pretreated with different concentrations of ibrutinib or DMSO for 30 minutes and then stimulated with  $\alpha$ CD3 or  $\alpha$ CD3 plus  $\alpha$ CD28 antibodies. Proliferation as measured by CFSE dilution after 48 hours was analyzed by flow cytometry in viable, 7-AAD-negative, single CD8<sup>+</sup> T-cells. **C)** PBMCs from healthy donors (n=3) were labeled with CFSE, pretreated with different concentrations of ibrutinib or DMSO for 30 minutes and then stimulated with  $\alpha$ CD3 or  $\alpha$ CD3 plus  $\alpha$ CD28 antibodies. Proliferation as measured by CFSE dilution after 72 hours was analyzed by flow cytometry in viable, 7-AAD-negative, single CD8<sup>+</sup> T-cells.

Graphs show means  $\pm$  SEM. MFI = median fluorescence intensity

**Figure 5: Blocking PD-1/PD-L1 axis enhances the anti-leukemic activity of ibrutinib**

C57BL/6 mice were transplanted with splenocytes from leukemic TCL1 mice, and after two weeks assigned to treatment with isotype antibody plus vehicle (control),  $\alpha$ PD-1,  $\alpha$ PD-L1, ibrutinib,  $\alpha$ PD-1 + ibrutinib, or  $\alpha$ PD-L1 + ibrutinib. Mice were sacrificed after 4 weeks of treatment (n=6). **A)** Absolute numbers of CD5<sup>+</sup>CD19<sup>+</sup> CLL cells in peripheral blood over time analyzed by flow cytometry, and **B)** spleen weight of different treatment arms at the end-point (n=6). **C)** Tumor load, defined as percentage of CD5<sup>+</sup>CD19<sup>+</sup> CLL cells out of CD45<sup>+</sup> cells in bone marrow (BM) (n=4-6).

Graphs show means  $\pm$  SEM. \*p<0.05, \*\*p<0.01, \*\*\*p<0.001

**Figure 6: Blocking PD-1/PD-L1 axis expands the effector population and enhances the functional capacity of CD8<sup>+</sup> T-cells**

C57BL/6 mice were transplanted with splenocytes from leukemic TCL1 mice, and after two weeks assigned to treatment with isotype antibody plus vehicle (control),  $\alpha$ PD-1, ibrutinib, or  $\alpha$ PD-1 + ibrutinib. Mice were sacrificed after 4 weeks of treatment. **A)** Flow cytometric analysis of splenic CD3<sup>+</sup>CD8<sup>+</sup> T-cells from different treatment arms (n=4). Cell subsets were defined as naïve (CD127<sup>hi</sup>CD44<sup>low</sup>), memory (Mem; CD127<sup>hi</sup>CD44<sup>hi</sup>) and effector (Eff; CD127<sup>low</sup>CD44<sup>int-hi</sup>) cells. **B)** Flow cytometric analysis of CD69 expression. **C-D)** Cytotoxic function of CD8<sup>+</sup> T-cells was assessed by flow cytometric analysis of **C)** degranulation capacity, as measured by CD107a expression on the cell surface, and **D)** IFN $\gamma$  production (n=4).

Graphs show means  $\pm$  SEM. \*p<0.05, \*\*\*p<0.001

# Figure 1

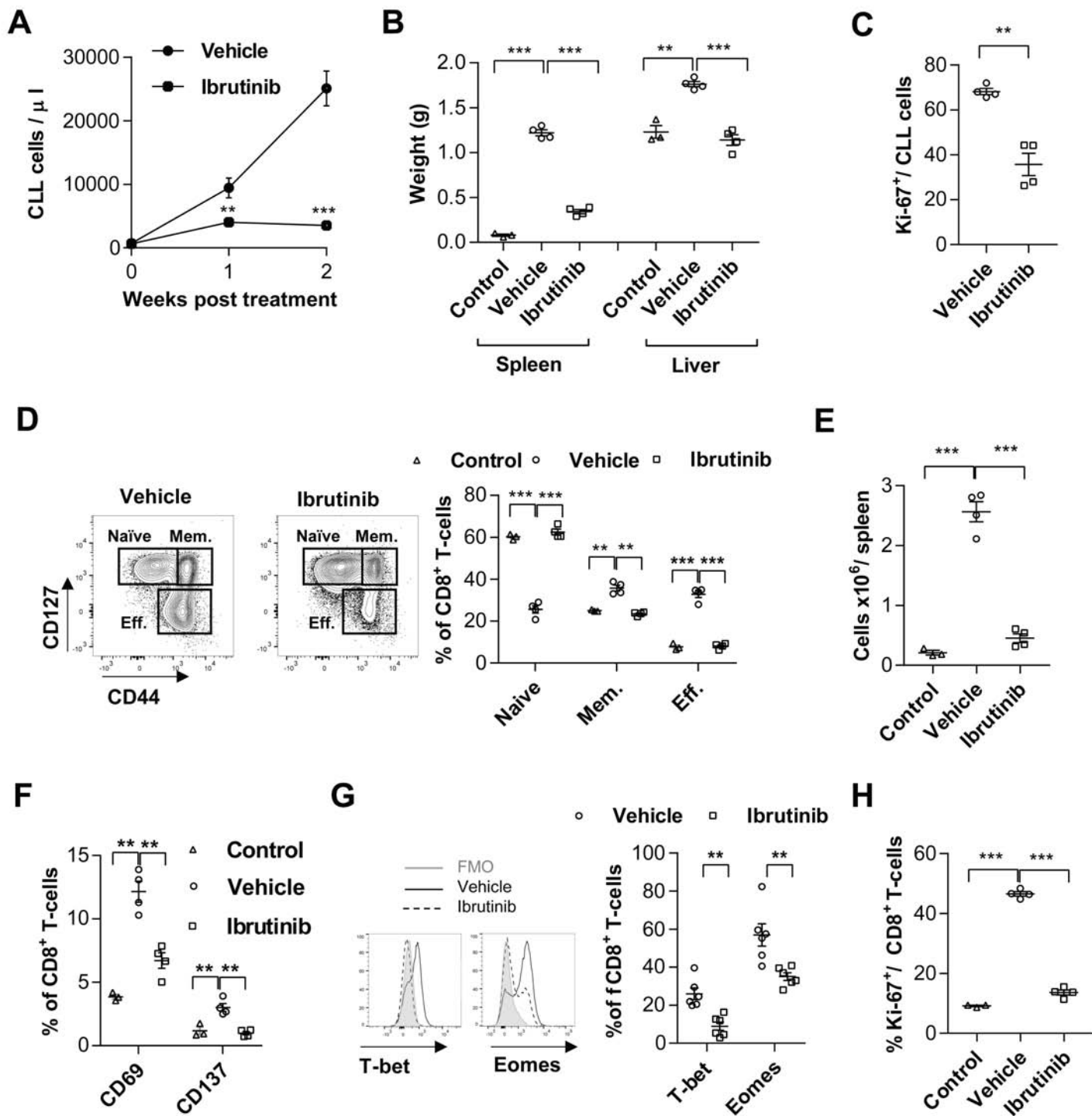


# Figure 2

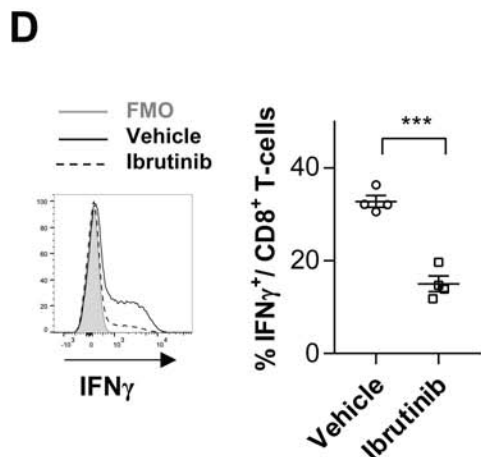
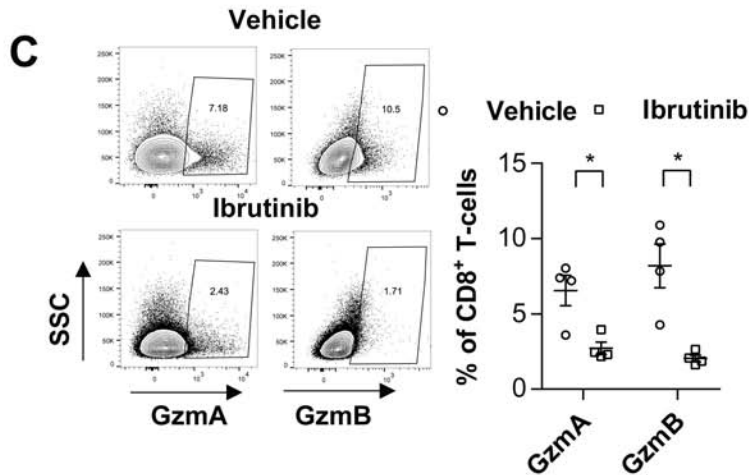
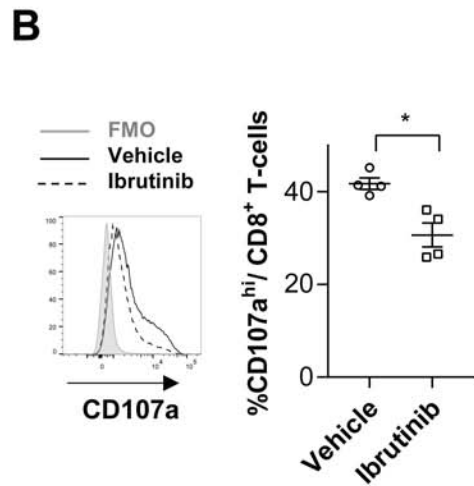
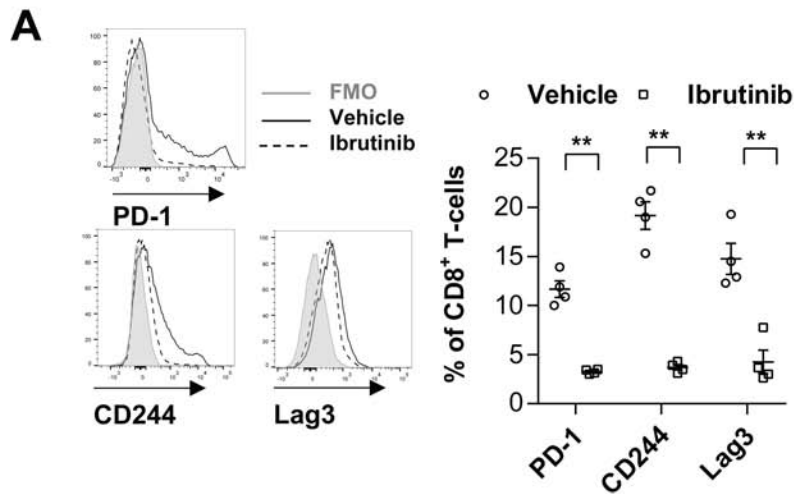
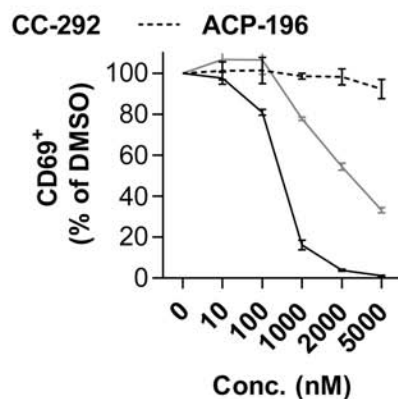
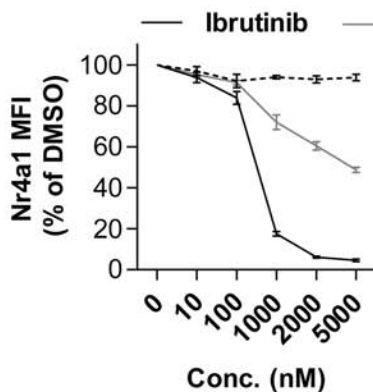
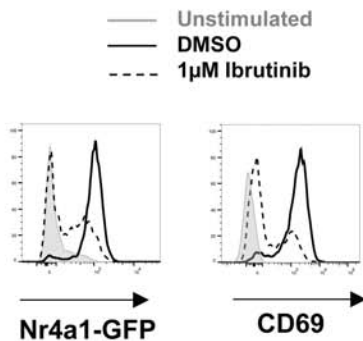
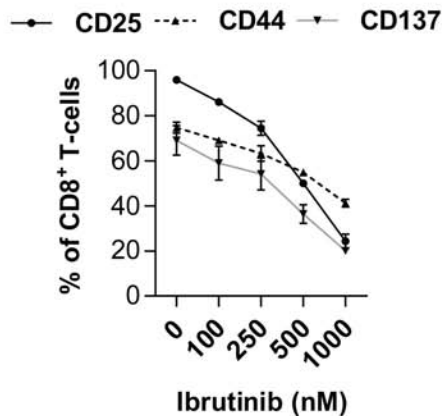


# Figure 3

**A**



**B**



**C**

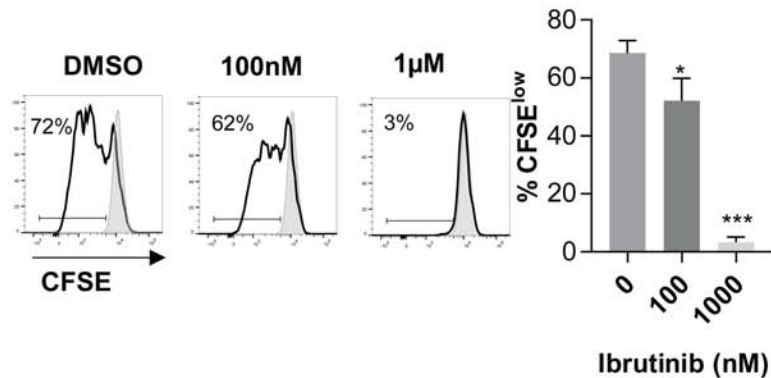
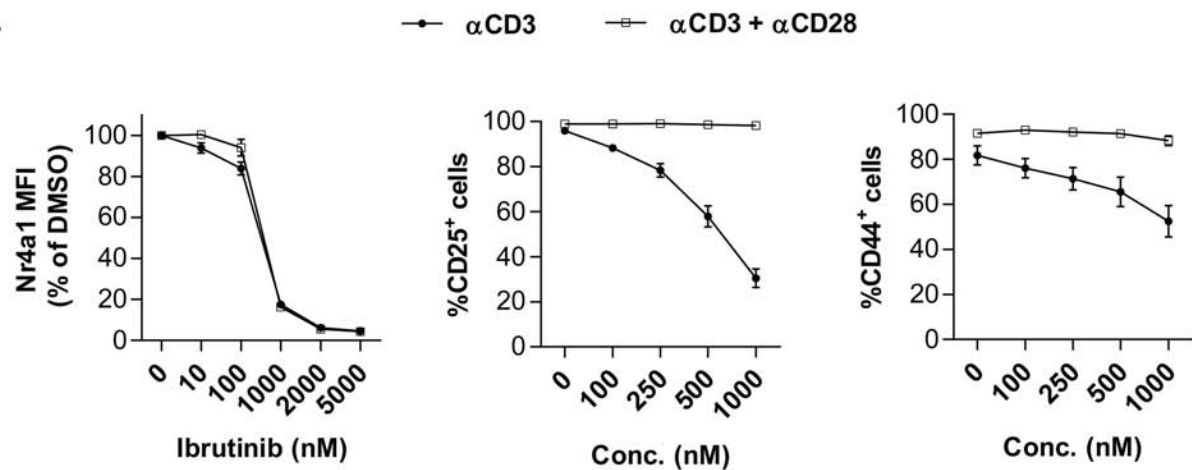
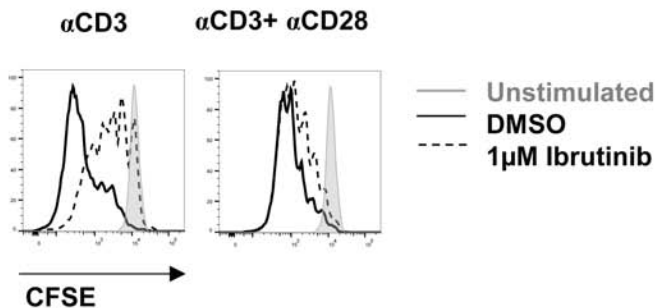


# Figure 4

## A



## B



## C

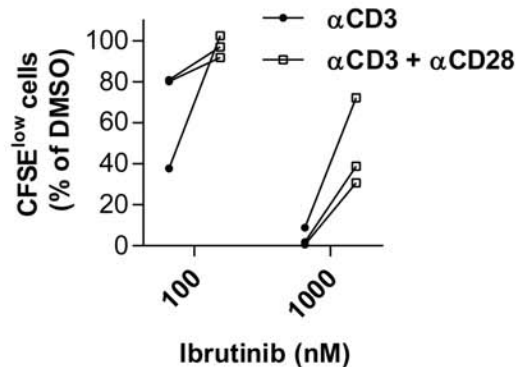
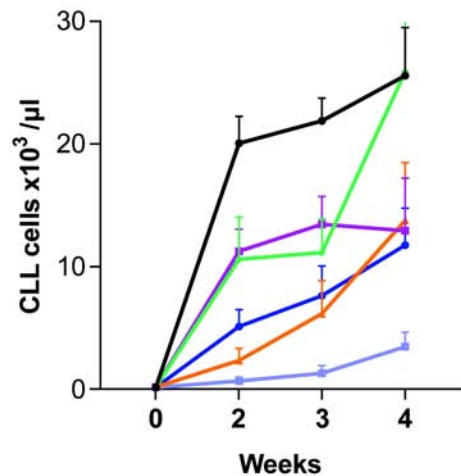
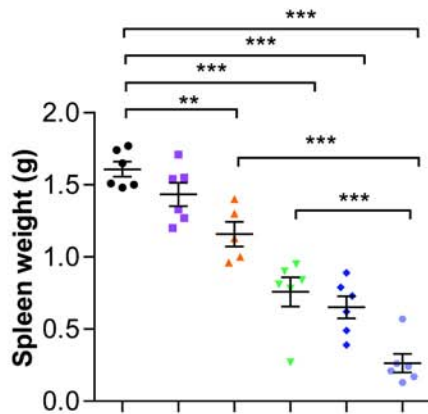


# Figure 5

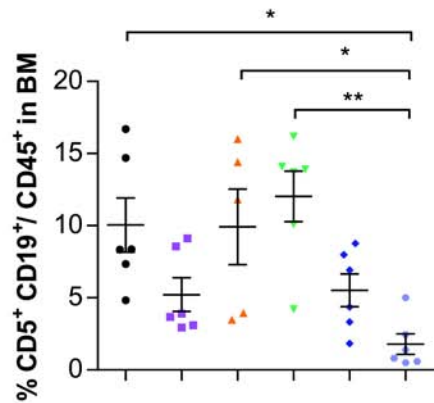
## A



## B



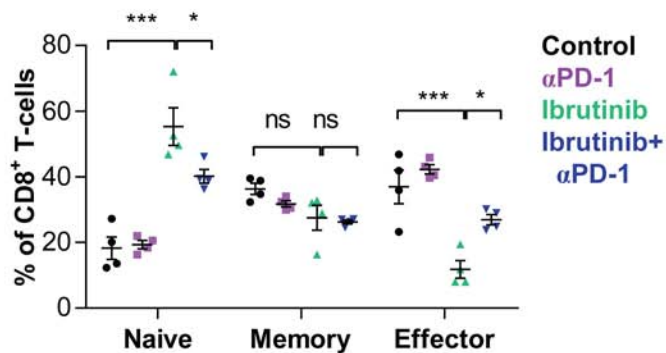
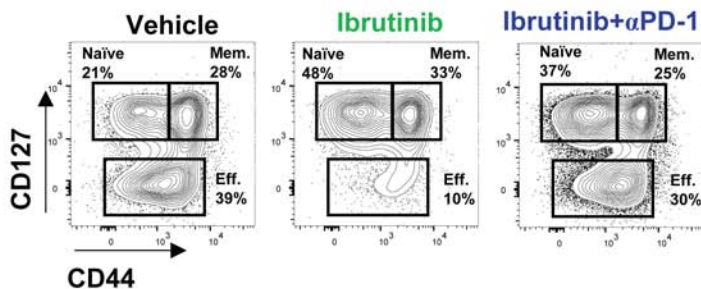
## C



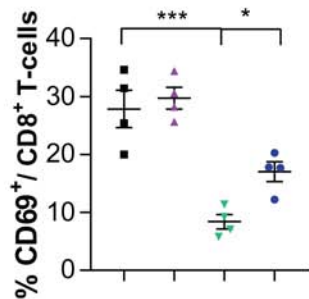
Control   αPD-1   αPD-L1   Ibrutinib   Ibrutinib+αPD-1   Ibrutinib+αPD-L1

# Figure 6

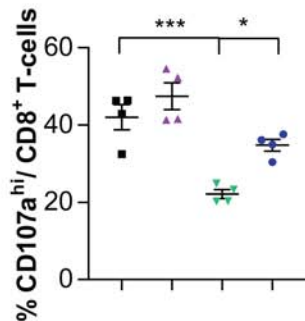
## A



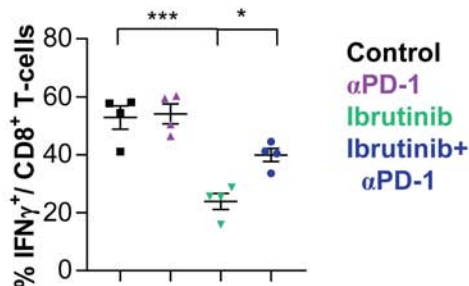
## B



## C



## D



## Supplementary Material and Methods

### Flow cytometry and functional testing

After preparation of single cell suspensions as described before,<sup>(1)</sup> cells were incubated with recommended dilutions of antibodies against cell surface proteins in PBS containing 0.1% fixable viability dye (eBioscience, Frankfurt am Main, Germany) for 30 minutes at 4°C. Cells were fixed using IC fixation buffer (eBioscience), washed and stored at 4°C in the dark until analyzed by flow cytometry.

For labelling of cells in whole blood, 50-100 µl of PB were stained with antibodies specific for surface molecules for 30 minutes at 4°C, followed by incubation for 10 minutes with 2 ml of 1X BD FACS™ lysing solution (BD Biosciences, Heidelberg, Germany) to remove erythrocytes. After centrifugation, supernatants were carefully aspirated and pelleted cells were resuspended in 150 µl of 1X BD FACSLysing solution. 50 µl of 123count eBeads™ (eBioscience, Frankfurt am Main, Germany) were directly added before data acquisition. Absolute cell numbers in blood were calculated according to the formula: absolute count (cells/µL) = (cell count x bead volume x bead concentration) / (bead Count x cell Volume).

For transcription factor staining, cells were fixed after surface molecule staining with FoxP3 fixation/permeabilization buffer (eBioscience) for 30 minutes at room temperature, followed by permeabilization with 1X permeabilization buffer (eBioscience) and staining with antibodies against transcription factors or IL-10 in 1X permeabilization buffer for 30 minutes at room temperature. After washing twice with 1X permeabilization

buffer, cells were resuspended in a final volume of 200  $\mu$ l 1X permeabilization buffer and stored at 4°C in the dark until analyzed by flow cytometry.

Cytokine release, granzyme B production and degranulation capacity of CD8<sup>+</sup> T-cells were assayed as previously described with minor modifications.(2) Cells were resuspended in complete medium (DMEM supplemented with 10% FCS, 10 mM HEPES, 1 mM sodium pyruvate, 0.1%  $\beta$ -mercaptoethanol, 100 U/ml penicillin, and 100  $\mu$ g/ml streptomycin), and seeded at a density of  $3 \times 10^6$  cells/200  $\mu$ l. Cells were incubated in cell stimulation cocktail in the presence of protein transport inhibitor cocktail (both from eBioscience) for 6 hours at 37 °C/ 5% CO<sub>2</sub>. Degranulation capacity of T-cells was measured by adding fluorochrome-conjugated anti-CD107a antibody (eBioscience) to the culture as previously described.(3) Afterwards, cells were washed, stained for surface proteins and fixed using IC fixation buffer (eBioscience). After washing with 1X permeabilization buffer, cells were stained with fluorescently labelled antibodies against intracellular proteins for 30 min at room temperature in the dark, washed and analyzed by flow cytometry.

For all flow cytometric measurement, data acquisition was done using BD LSRII or BD FACSCanto flow cytometer (BD Biosciences). Median Fluorescence Intensity (MFI) was recorded and normalized by subtracting the MFI of the respective fluorescence-minus-one (FMO) control. Data analysis was performed using FlowJo X 10.0.7 software (FlowJo, Ashland, OR, USA).

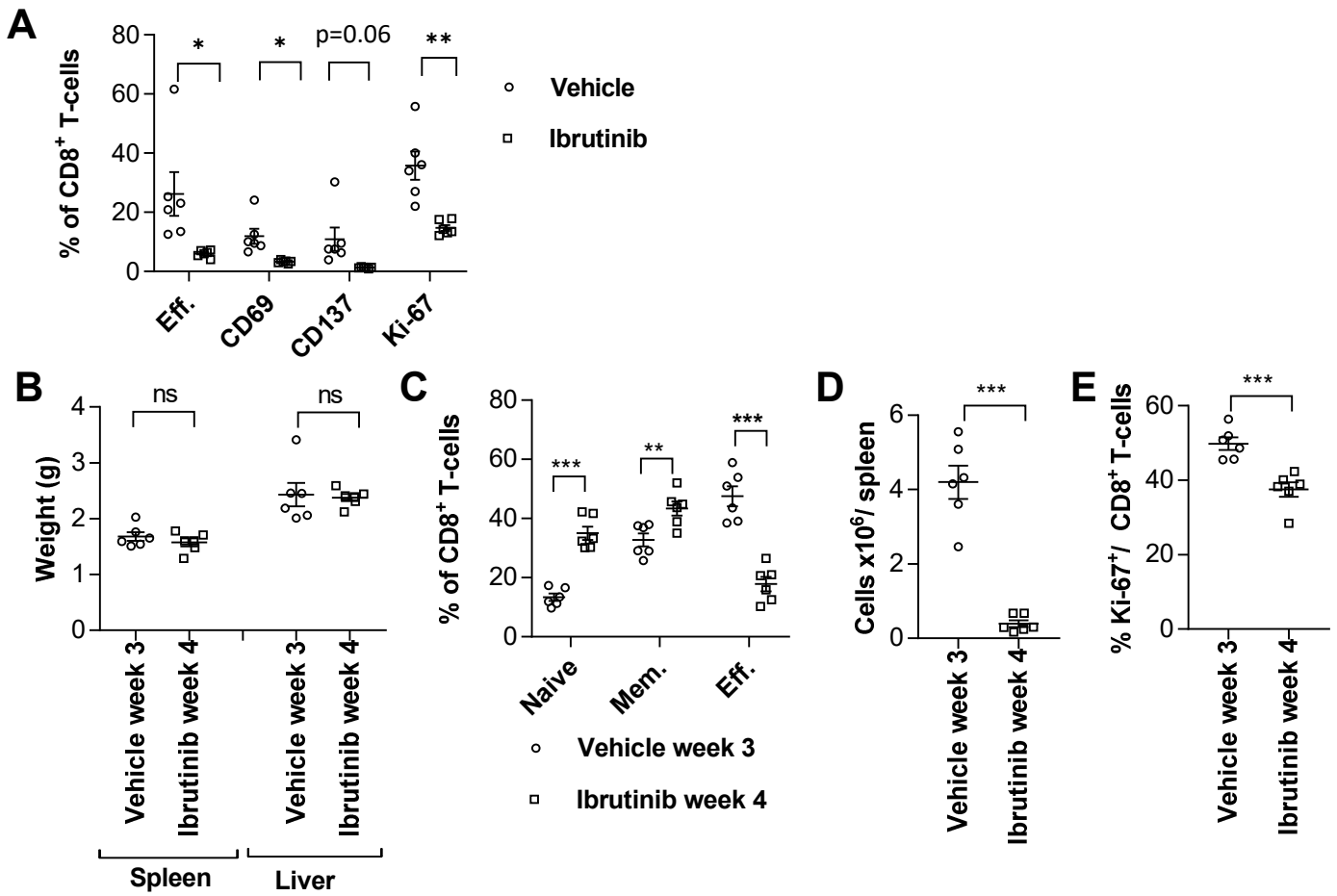
## References

1. Haderk F, Schulz R, Iskar M, Cid LL, Worst T, Willmund KV, et al. Tumor-derived exosomes modulate PD-L1 expression in monocytes. *Science Immunology*. 2017;2(13).
2. McClanahan F, Hanna B, Miller S, Clear AJ, Lichter P, Gribben JG, et al. PD-L1 Checkpoint Blockade Prevents Immune Dysfunction and Leukemia Development in a Mouse Model of Chronic Lymphocytic Leukemia. *Blood*. 2015;126(2):203-11.
3. Betts MR, Brenchley JM, Price DA, De Rosa SC, Douek DC, Roederer M, et al. Sensitive and viable identification of antigen-specific CD8+ T cells by a flow cytometric assay for degranulation. *J Immunol Methods*. 2003 Oct 01;281(1-2):65-78.

### Supplementary Table 1: List of flow cytometry antibodies

Mouse antibodies	Clone	Supplier
anti-mouse CD107a (LAMP-1)	eBio1D4B	eBioscience
anti-mouse CD19	eBio1D3	eBioscience
anti-mouse CD19	6D5	Biolegend
anti-mouse CD3e	145-2C11	eBioscience
anti-Mouse CD3e	500A2	BD
anti-mouse CD4	GK1.5	Biolegend
anti-mouse CD4	RM4-5	eBioscience
anti-mouse CD44	IM7	eBioscience
anti-mouse CD45	30F-11	Biolegend
anti-mouse CD5	53-7.3	BD
anti-mouse CD69	H1.2F3	Biolegend
anti-mouse CD8a	53-6.7	Biolegend
anti-mouse CD127	A7R34	Biolegend
Anti-mouse CD137	17B5	Biolegend
anti-mouse CD62L	MEL-14	eBioscience
anti-mouse CD25	PC-61	Biolegend
anti-mouse Granzyme B	NGZB	eBioscience
anti-mouse IFNg	XMG1.2	eBioscience
anti-mouse GITR	YGL 386	Biolegend
anti-mouse Lag3	eBioC9B7W	eBioscience
anti-mouse PD-1	RMP1-30	Biolegend
anti-mouse CD244	m2B4 (B6)458.1	Biolegend
anti-mouse Ki67	SolA15	eBioscience
anti-mouse Eomes	Dan11mag	eBioscience
anti-T-bet	4B10	Biolegend

# Supplementary Figure 1

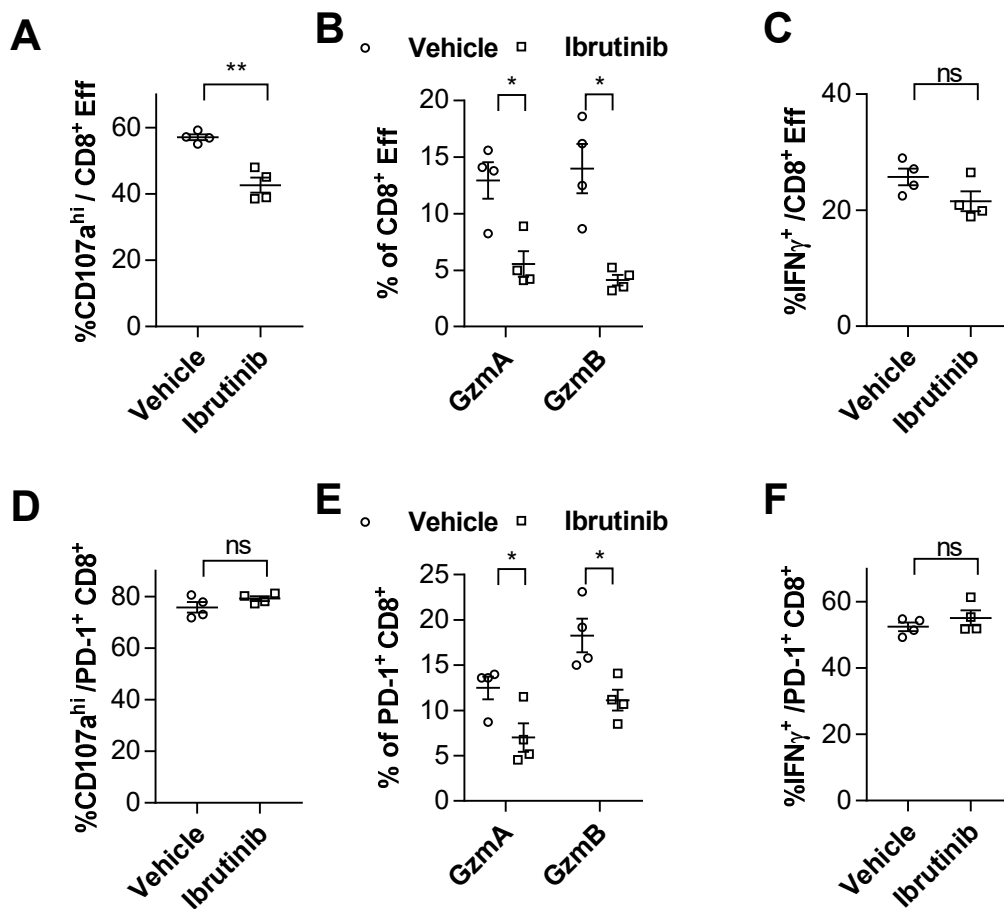


## Supplementary Figure 1: Ibrutinib modulates effector CD8<sup>+</sup> T-cell differentiation and proliferation in the TCL1 adoptive transfer model

C57BL/6 mice were transplanted with splenocytes from leukemic TCL1 mice, and later assigned to treatment with ibrutinib (0.16 mg/mL) or vehicle control in drinking water. **A**) Treatment started when all mice reached the leukemic threshold (5,000 CLL cells/ $\mu$ L of blood). Graph shows the impact of the treatment on CD8<sup>+</sup> T-cell effector population, activation and proliferation. **B-E**) Vehicle- and ibrutinib-treated mice were sacrificed after 3 and 4 weeks of treatment, respectively, when mice reached disease end-stage. **B**) Spleen and liver weight of vehicle- or ibrutinib-treated mice (n=5). **C**) Flow cytometric analysis of splenic CD3<sup>+</sup>CD8<sup>+</sup> T-cell subsets from vehicle- or ibrutinib-treated mice (n=5-6). **D**) Absolute numbers of splenic CD8<sup>+</sup> effector cells from vehicle- or ibrutinib-treated mice (n=5-6) were assessed by flow cytometry. **E**) Flow cytometric analysis of Ki-67 expression in CD8<sup>+</sup> T-cells from vehicle- or ibrutinib-treated mice (n=5-6).

Graphs show means  $\pm$  SEM. \*p<0.05, \*\*p<0.01, \*\*\*p<0.001, ns = not significant

## Supplementary Figure 2

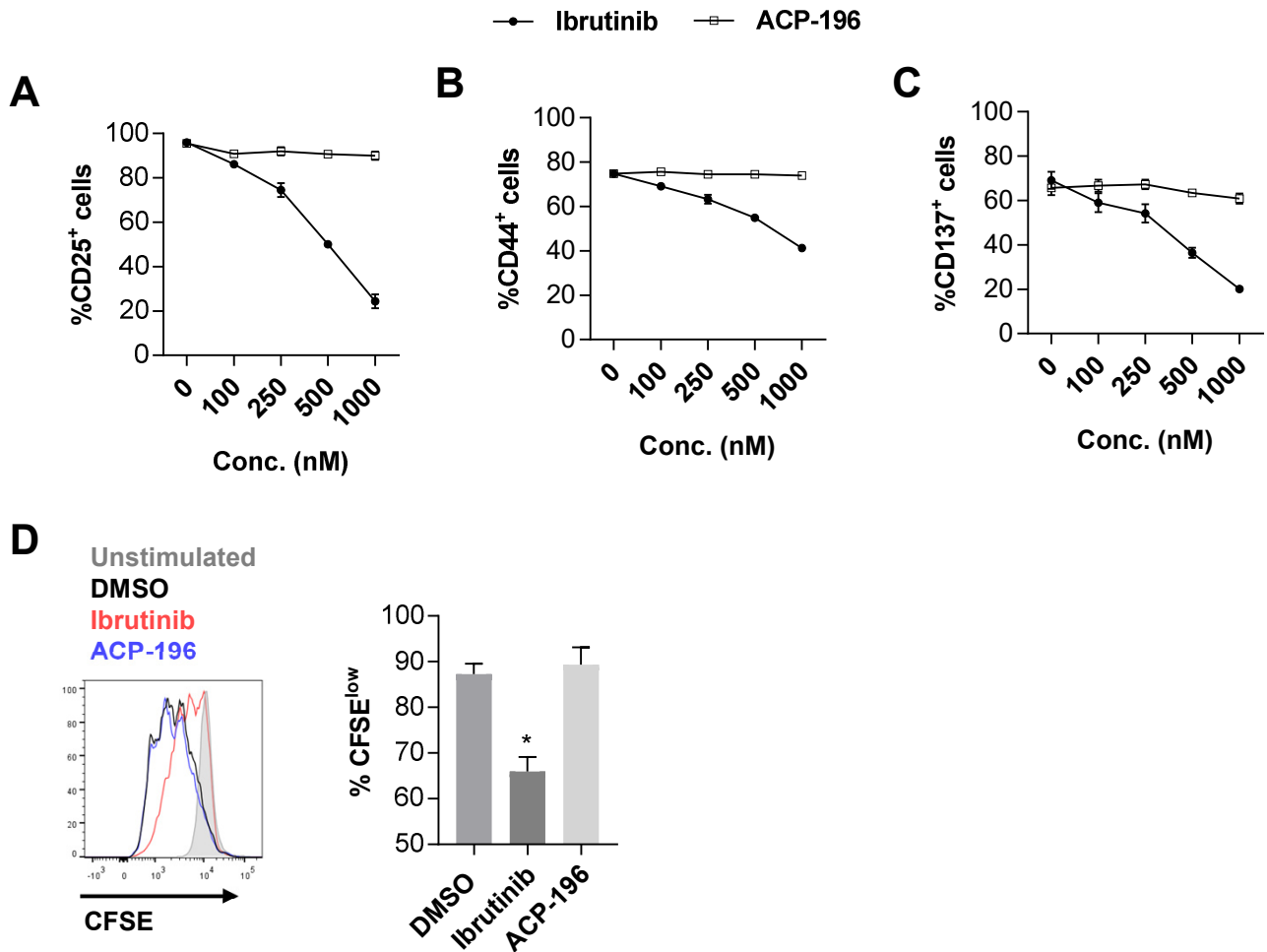


### Supplementary Figure 2: Ibrutinib modulates CD8<sup>+</sup> T-cell function in the TCL1 adoptive transfer model

C57BL/6 mice were transplanted with splenocytes from leukemic TCL1 mice, and after two weeks assigned to treatment with ibrutinib (0.16 mg/mL) or vehicle control in drinking water. Mice were sacrificed after 2 weeks of treatment. **A-C)** Cytotoxic function of CD8<sup>+</sup> effector T-cells, and **D-F)** of PD-1<sup>+</sup>CD8<sup>+</sup> T-cells was assessed by flow cytometric analysis of degranulation capacity, as measured by CD107a expression on the cell surface, GzMA and GzMB expression or IFN<sub>γ</sub> production (n=4).

Graphs show means ± SEM. \*p<0.05, \*\*p<0.01, ns = not significant; nMFI = normalized median fluorescence intensity

## Supplementary Figure 3

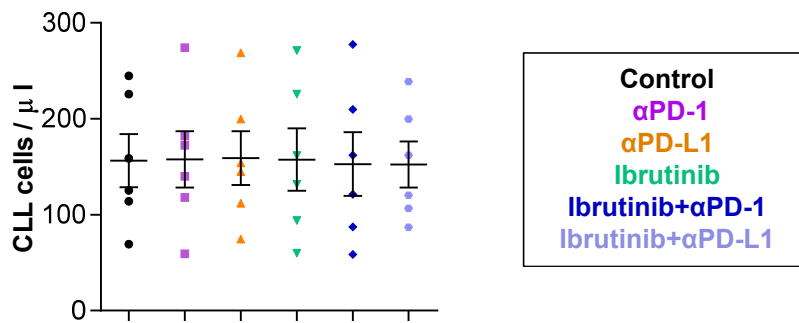


### Supplementary Figure 3: Ibrutinib modulates T-cell receptor signaling in CD8<sup>+</sup> T-cells

**A-C)** Splenocytes from C57BL/6 mice (n=4) were pretreated with different concentrations of ibrutinib, ACP-196 or DMSO for 30 minutes and then stimulated with anti-CD3 antibody. CD25, CD44 and CD137 expression were analyzed by flow cytometry in viable, 7-AAD-negative, single CD8<sup>+</sup> T-cells after 24 hours. **D)** Splenocytes from C57BL/6 mice (n=4) were labeled with 5  $\mu$ M CFSE, pretreated with 1  $\mu$ M of ibrutinib, ACP-196 or DMSO for 30 minutes, and then stimulated with anti-CD3 antibody. Proliferation as measured by CFSE dilution after 48 hours was analyzed by flow cytometry in viable, 7-AAD-negative, single CD8<sup>+</sup> T-cells.

Graphs show means  $\pm$  SEM. \*p<0.05; MFI= median fluorescence intensity

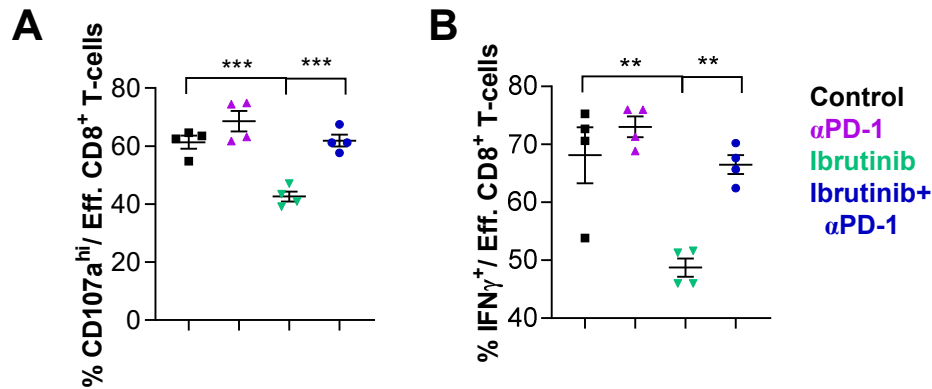
## Supplementary Figure 4



### Supplementary Figure 4: Blocking PD-1/PD-L1 axis enhances the anti-leukemic activity of ibrutinib

C57BL/6 mice were transplanted with splenocytes from leukemic TCL1 mice, and after two weeks assigned to treatment with isotype antibody plus vehicle (control),  $\alpha\text{PD-1}$ ,  $\alpha\text{PD-L1}$ , ibrutinib, ibrutinib +  $\alpha\text{PD-1}$ , or ibrutinib +  $\alpha\text{PD-L1}$ . Graph shows the absolute numbers of CD5<sup>+</sup>CD19<sup>+</sup> CLL cells in peripheral blood prior to treatment.

## Supplementary Figure 5



### Supplementary Figure 5: Blocking PD-1/PD-L1 axis expands the effector population and enhances the functional capacity of CD8<sup>+</sup> T-cells

C57BL/6 mice were transplanted with splenocytes from leukemic TCL1 mice, and after two weeks assigned to treatment with isotype antibody plus vehicle (control),  $\alpha$ PD-1, ibrutinib, or ibrutinib +  $\alpha$ PD-1. Mice were sacrificed after 4 weeks of treatment. Cytotoxic function of CD8<sup>+</sup> effector T-cells was assessed by flow cytometric analysis of **A**) degranulation capacity, as measured by CD107a expression on the cell surface, and **B**) IFN $\gamma$  production (n=4).

Graphs show means  $\pm$  SEM. \*\*p<0.01, \*\*\*p<0.001